Comparative study of uplink and downlink beamforming algorithms in UTRA/TDD

Benoît Pelletier, Jian Mao and Benoît Champagne
Department of Electrical and Computer Engineering, McGill University
3480 University, Montréal, Québec, Canada H3A 2A7
{bpelle,mao}@tsp.ece.mcgill.ca, champagne@ece.mcgill.ca

Abstract— **The arrival of new multi-media and Internet services to mobile cellular subscribers has led to the development of new techniques, such as antenna array or smart antennas (SA), to improve spectrum efficiency. SA provides a means for spatial filtering for separating users based on angular characteristics, a method also known as beamforming. In this contribution, the performance of various beamforming algorithms is studied for the uplink and downlink of a UTRA/TDD system under realistic deployment and channel models. The algorithms are evaluated in terms of improvement in signal to interference plus noise ratio (SINR) and coded bit error rate (BER) with RAKE receiver structure and compared to a more complex space-time multi-user detection receiver. We consider three different beamforming algorithms, namely: switched beams (SB), dynamically phased arrays (DPA) and sample matrix inversion (SMI). The results indicate that on the uplink, SMI has the potential to perform better than both DPA and SB but DPA outperforms both SB and SMI on the downlink.**

I. Introduction

The arrival of new multi-media and Internet services to mobile cellular subscribers will create an important demand for radio bandwidth. This demand for the scarce radio resources has led to the development of new techniques to improve spectrum efficiency such as multi-user detection (MUD), dynamic capacity allocation (DCA), and antenna array or smart antennas (SA). The latter provides a spatial filtering means for separating users based on angular characteristics, also known as space division multiple access (SDMA). Filtering in the spatial domain allows the separation of spectrally and temporally overlapping signals possibly originating from different users with unique spatial signatures. In addition to reducing interference, a definite advantage for wideband code division multiple access (WCDMA) systems, it can also allow the same channel (frequency, *timeslot* or code) to be allocated to different users in the same cell, effectively increasing spectral efficiency. For these reasons, SA is considered a key technology for capacity increase for present and future wireless cellular systems.

Earlier studies have shown that SA has the potential to significantly increase the capacity of WCDMA cellular systems (e.g. [1], [2]). While a number of those studies focus on the uplink, few considered the downlink. For 3G and future generation systems (B3G, 4G, etc.), most of the data traffic (e.g. multi-media, Internet, etc.) is to be carried on the downlink. To get a complete picture, it is essential that both directions be considered.

In this contribution, the performance of beamforming algorithms based on switched beams (SB), dynamically phased arrays (DPA), and sample matrix inversion (SMI) on the uplink and downlink of a UTRA/TDD system are evaluated under realistic deployment conditions.

This paper is organized as follows. Section II presents some background information on UTRA/TDD and introduces the system model. The algorithms, devised to exploit the structure of UTRA/TDD and to take advantage of the channel reciprocity in TDD mode are presented in Section III. Results, including the average signal to interference plus noise (SINR) and coded bit error rate (BER) for the studied systems are then shown in Section IV. Section V concludes the article, summarizing the findings.

II. Background

A. UTRA/TDD

The UTRA/TDD physical layer (see [3], [4]) uses CDMA as multiple access technique combined with time division duplexing (TDD) for separating the uplink and downlink transmission. Time is divided into 10ms frames each containing 15 *timeslots* as illustrated in Fig. 1. A radio resource is therefore identified by both a code and a timeslot index.

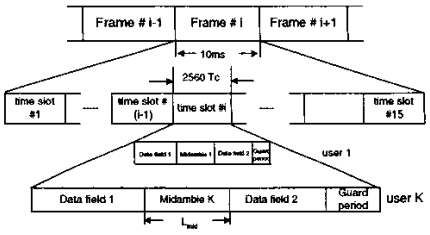

Fig. 1
UTRA/TDD Frame Structure

The timeslots in the 3.84Mcps option contain 2560 chips of duration T_c. Each timeslot within a frame can be used for either uplink or downlink transmission with the restriction that a frame must include at least one uplink and one downlink timeslot. This flexibility in the uplink/downlink arrangement in TDD/CDMA makes it an advantageous multiple access scheme for asymmetric traffic such as video, high quality audio, Internet traffic and others.

0-7803-8255-2/04/$20.00 ©2004 IEEE.

Each timeslot is further separated in four parts; two data fields separated by a midamble, and a guard period (GP) to terminate the timeslot. The data fields carry the data bits destined to upper layer after multiplexing, coding, interleaving, spreading and scrambling. The midamble is a known sequence of chips used for channel estimation and training. The guard period is a time interval during which transmission is halted; it separates two subsequent timeslots to prevent overlap in dispersive channels.

Spreading and modulation is performed as illustrated in Fig. 2. Coded data bits are first grouped in pairs to form a complex data symbol. Then, the complex data symbols are weighted by a channelization code multiplier w_k. The latter depends on the specific orthogonal variable spreading factor (OVSF) code $\mathbf{c}_k \in \mathbb{C}^Q$ with processing gain $Q \in \{1, 2, 4, 8, 16\}$. Once the data symbols are spread with the OVSF channelization code, they are then scrambled at the chip rate by the cell-specific scrambling code $\mathbf{s}_c \in \mathbb{C}^{Q_{\max}}$, $Q_{\max} = 16$. The scrambled data symbols are finally QPSK modulated with a root raised cosine pulse shaping function.

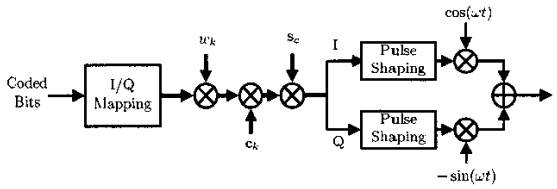

Fig. 2
UTRA/TDD SPREADING AND MODULATION

B. System model

To simplify, we consider the case where all cells have the same frame structure (i.e. all the base stations are on the uplink (or downlink) simultaneously), however more general cases can easily be studied. For the uplink, we consider the sampled baseband received signal vector at one particular sector. Let $\mathbf{x}(n) \in \mathbb{C}^M$ be the sampled baseband received signal vector at the antenna array output of the *sector of interest* (SOI), where M is the number of elements in the array. Then $\mathbf{x}(n)$ for $0 \leq n \leq T_{ts}$, there T_{ts} is the length of the timeslot in number of chips, consists of the sum of the contribution from all users in the system and noise:

$$\mathbf{x}(n) = \sum_{k} \sum_{l=0}^{L_k-1} \xi^u_{k,l} \mathbf{h}^u_{k,l}(n) s_k(n - \tau^u_{k,l}) + \mathbf{w}(n), \quad (1)$$

where L_k is the number of paths from user k to the SOI, $s_k(n)$ is the transmitted signal from user k, $\xi^u_{k,l}$, $\mathbf{h}^u_{k,l}(n)$ and $\tau^u_{k,l}$ are the uplink gain, normalized vector channel coefficient and delay for the path l of user k to the SOI, respectively, and $\mathbf{w}(n)$ is the AWGN noise term ($E[\mathbf{w}(n)\mathbf{w}^H(n)] = \sigma_u^2 \mathbf{I}$). Synchronization among the users belonging to the same sector is assumed.

Similarly for the downlink, we consider the baseband signal $x(n) \in \mathbb{C}$ received at a particular mobile in the SOI, called the *mobile of interest* (MOI). The received signal consists of the contribution of the downlink signal from all sectors in the system that are transmitting to their respective mobiles, and AWGN noise:

$$x(n) = \sum_{i \in \mathcal{S}} \sum_{l=0}^{L_i-1} \xi^d_{i,l} \sum_{k \in \mathcal{K}_i} \mathbf{w}^H_{k,i} \mathbf{h}^d_{i,l}(n) s_{k,i}(n - \tau^d_{i,l}) + w(n), \quad (2)$$

where $\mathcal{S}$ is the set of all sectors in the system, L_i is the number of paths from the sector i to the MOI, $\mathcal{K}_i$ is the set of all users that belong to sector i, $\mathbf{w}_{k,i}$ is the weight vector for the downlink of user k in sector i, $\xi^d_{i,l}$, $\mathbf{h}^d_{i,l}(n)$ and $\tau^d_{i,l}$ are the downlink gain, normalized vector channel coefficient and time delay for path index l from sector i to the MOI, respectively, and finally $w(n)$ is the AWGN noise term with $E[w(n)w^*(n)] = \sigma_d^2$.

It is assumed in (1) and (2) that the guard period is long enough so that the contribution of signal leaks from other timeslots is negligible. The baseband transmitted signal for user k in sector i is normalized so that $|s_{k,i}(n)|^2 = 1$.

The time-varying vector channel coefficients, $\mathbf{h}^u_{k,l}(n)$ and $\mathbf{h}^d_{i,l}(n)$ in (1) and (2), respectively, are modeled as a linear superposition of propagation path contributions associated to a continuum of direction of arrival (DOA), Doppler angles and propagation delays as proposed in [5]. They are obtained via the application of an efficient space-time correlation shaping transformation on an independent random sequence. With the help of this vector channel simulator, the spatio-temporal characteristics of the channel are appropriately replicated.

Beamforming is performed as illustrated by the generic block diagram in Fig. 3. A set of weight vectors is first calculated from the array received signal according to one of the algorithm presented in the next section. Then, each weight vector is applied to the array output and the resulting set of signals are combined and demodulated with a RAKE receiver.

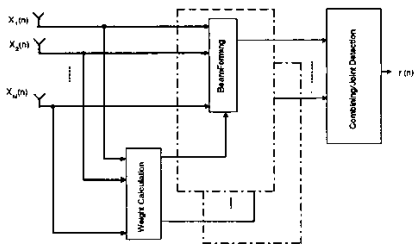

Fig. 3
GENERIC BEAMFORMING BLOCK DIAGRAM

III. ALGORITHMS

A. Switched beam

In the switch beam method, a set of fixed antenna array beams are "steered" in discrete angular steps, spatially covering the entire sector[1]. In practice, this can be implemented at baseband using pre-defined antenna weights or at intermediate-frequency (IF) using phase-shifters. In the former case, the

output $r_l(n)$ of the l^{th} beam on the uplink is obtained by applying a fixed set of weights $\mathbf{w}_l$ to the antenna array, i.e.:

$$r_l(n) = \mathbf{w}_l^H \mathbf{x}(n), \quad l \in \{0, \ldots, B-1\}, \tag{3}$$

where B sets of pre-defined weights are available.

As illustrated in Fig. 3, one or more beams may be selected for the incoming signal of a particular user to increase its signal strength and reduce its interference level. We focus on two different approaches for SB, namely the best beam (SB-BB) and the maximal ratio combining (SB-MRC) approach. For both methods, the SINR for the user of interest is measured at the output of each fixed beam. In the SB-BB approach, the beam with the best SINR is selected for demodulation, i.e.:

$$l_b = \arg\max_l \gamma_{k,l}, \tag{4}$$

where l_b is the best beam index and $\gamma_{k,l}$ is the SINR for user k on beam l. Then the output of the SB-BB becomes $r_{\text{BB}}(n) \triangleq r_{l_b}(n)$. For the SB-MRC approach, a combination of two or more beams is used for demodulation, and the output $r_{\text{MRC}}^{(k)}(n)$ for the user k can be expressed as

$$r_{\text{MRC}}^{(k)}(n) = \sum_{l \in \mathcal{B}_k} \alpha_{k,l}^* r_l(n), \tag{5}$$

where $\mathcal{B}_k$ denotes the set of the $N_b \leq B$ best beams in the SINR sense to which MRC is applied and $\alpha_{k,l}$ is the MRC coefficient for user k, obtained from the complex gain estimate of the l^{th} beam output.

For the downlink, assuming reciprocity in the spatial channel, the weight vector is selected as in (4) for SB-BB. For SB-MRC, each of the N_b best beams transmit information and the fraction of power allocated to each beam is set to be proportional to the fraction of the uplink power received on that beam for the user of interest, normalized with respect to the total power received for that user on the N_b best beams. Specifically, if we let $P_{k,b}$ denote the received power at beam b for user k, then the fraction $Q_{k,b}$ of power transmitted on each downlink beam is given by

$$Q_{k,b} = \frac{P_{k,b}}{\sum_{b' \in \mathcal{B}_k} P_{k,b'}}. \tag{6}$$

For both SB-BB and SB-MRC cases, the transmit power is adjusted so that the target level at the user k is achieved.

B. Dynamically phased array

The DPA can be interpreted as an extended SB system where it is possible to steer the beams toward a continuum of DOA. The beams are steered by adjusting the phases of the signals at each antenna array elements while keeping the weights amplitude fixed.

In this method, also called conventional beamforming [6], the weights on the uplink are calculated based on the estimated DOAs of the user dominant signal paths. The proposed DPA beamforming procedure therefore includes two steps: direction of arrival estimation (e.g. [7], [8], [9]) and weight computation. As in the SB case, one or more set of weights can be used to combine multiple signal paths.

Let $\mathbf{a}(\theta)$ denote the array propagation vector, defined as the array response to a plane wave impinging from angle θ with respect to broadside. For a M-elements uniform linear array (ULA) with inter-spacing d, the array propagation vector is given by $\mathbf{a}(\theta) = [1, \exp(-j2\pi d \sin\theta), \ldots, \exp(-j2\pi d(M-1)\sin\theta)]^T$. Then the set of DPA weights used for path l of user k are calculated to match the array propagation vector and normalized to have unit power in the estimated look direction $\widehat{\theta}_{k,l}$ i.e.:

$$\mathbf{w}_{k,l} = \mathbf{a}(\widehat{\theta}_{k,l}) \quad l \in \{0, 1, \ldots, L_k - 1\}, \tag{7}$$

where L_k is the number of time-differentiable paths (TDP) for user k. Notice that with DPA, the set of weights are in general different from user to user.

As in the case of SB, two possible methods of beam selection for DPA are studied, namely the best beam (DPA-BB) and maximal ratio combining (DPA-MRC) approach. The weight vector index l_b for DPA-BB can be obtained as in (4), i.e.:

$$l_b = \arg\max_l \gamma_{k,l} \quad l \in \{0, 1, \ldots, L_k - 1\}, \tag{8}$$

where $\gamma_{k,l}$ is the uplink SINR for user k measured at the output of beam l. The weight vector for DPA-BB then becomes $\mathbf{w}_{k,l_b} = \mathbf{a}(\widehat{\theta}_{k,l_b})$ and the beamformer output signal on the uplink is given by

$$r_{\text{BB}}^{(k)}(n) = \mathbf{w}_{k,l_b}^H \mathbf{x}(n). \tag{9}$$

For DPA-MRC, several beams are combined and in the same way as for DPA-SB, the beamformer output can be expressed as

$$r_{\text{MRC}}^{(k)}(n) = \sum_{l \in \mathcal{L}_k} \alpha_{k,l}^* \mathbf{w}_{k,l}^H \mathbf{x}(n), \tag{10}$$

where $\mathcal{L}_k$ is the set of $N_b \leq L_k$ path indices with best SINR metrics for user k and $\alpha_{k,l}$ is the MRC coefficient for user k and path l.

For the downlink, the same principles developed for the SB apply for DPA. As such, for DPA-BB the uplink weight vector is used on the downlink, and for DPA-MRC multiple weight vectors are linearly combined coherently according to the power received on each beam as in (6). The downlink power is adjusted so that the target level power is achieved at the mobile user.

C. Sample matrix inversion

In the sample matrix inversion (SMI) method, the beamforming weights are computed on the uplink based on the estimation of the array output covariance matrix and correlation vector between the reference and array received signals. The optimal weights are then obtained from the minimization of the mean square error (MMSE) of the cost function

$$J(\mathbf{w}_{k,l}) = E[|d_k(n - \tau_{k,l}^u) - \mathbf{w}_{k,l}^H \mathbf{x}(n)|^2], \tag{11}$$

where $d_k(n)$ is the reference signal for user k. It is well known that the optimal MMSE solution of (11) for user k and time-differentiable path l is given by

$$\mathbf{w}_{k,l}^o = \mathbf{R}_{xx}^{-1} \mathbf{r}_{k,l}, \tag{12}$$

where $\mathbf{R}_{xx} \triangleq E[\mathbf{x}(n)\mathbf{x}^H(n)]$ is the array covariance matrix and $\mathbf{r}_{k,l} \triangleq E[\mathbf{x}(n)d_k^*(n-\tau_{k,l}^u)]$ is the cross-correlation vector. In practice, both $\mathbf{R}_{xx}$ and $\mathbf{r}_{k,l}$ are unknown at the receiver and need to be estimated. In UTRA/TDD, two approaches can be used to estimate $\mathbf{r}_{k,l}$; the first approach uses the midamble as reference signal and the second uses the data fields in decision-feedback (DF) as reference. Similarly, $\mathbf{R}_{xx}$ can be estimated from the data fields and the midamble section.

It would seem natural in UTRA/TDD to use the entire timeslot for the estimation of the covariance matrix and the midamble section for the estimation of the cross-correlation vector. In a multipath environment however, it can be shown that in general, the true array covariance matrix $\mathbf{R}_{xx}$ in the midamble section and in the data fields are different. The same applies to the true cross-correlation vector $\mathbf{r}_{k,l}$ and this is due to the cross-correlation and auto-correlation properties of the midambles, which are very different than those of the signature sequences used in the data fields. Thus to obtain the optimum weights for data detection in a multipath environment, the data fields sections must be used to estimate $\mathbf{R}_{xx}$ and $\mathbf{r}_{k,l}$.

The sample matrix estimate of $\mathbf{R}_{xx}$ can be obtained from the array data as

$$\widehat{\mathbf{R}}_{xx} \triangleq \frac{1}{N_R} \sum_{n=i_R}^{i_R+N_R-1} \mathbf{x}(n)\mathbf{x}^H(n), \tag{13}$$

where N_R and i_R are the number of samples and the starting index of the observation interval for the covariance matrix, respectively. Similarly for the cross-correlation vector estimate:

$$\widehat{\mathbf{r}}_{k,l} \triangleq \frac{1}{N_r} \sum_{n=i_r}^{i_r+N_r-1} \mathbf{x}(n)d_k^*(n-\tau_{k,l}^u), \tag{14}$$

where $d_k(n)$ is the reference signal taken either in the midamble section or in the data field depending on the approach, N_r and i_r are the number of samples and the starting index of the observation interval for the cross-correlation vector, respectively. N_R, i_R, N_r, and i_r depend on the approach used for the estimation.

As for DPA and SB, the best beam (SMI-BB) and maximal ratio combining (SMI-MRC) approaches can be used. The only difference between DPA and SMI is the actual weight computation; equations (8)-(10) thus apply for SMI as well.

Reciprocity can be assumed for the channel in TDD but in general, it cannot be assumed for the interference. The spatial interference measured on the uplink is not a suitable measure of the interference at the mobile. Hence SMI is in general not appropriate for the downlink and will be considered only for completeness.

IV. Computer Experiments

A. Methodology

The simulation area consists of 7 hexagonal cells with 3 sectors each. To simplify the simulations, data is gathered only from one sector of the central cell, the *sector of interest* (SOI). The other sectors provide realistic spatial interference.

Parameter	Value (UL/DL)
Cell radius	200m
Number of antenna elements	8
Mobile velocity	15m/s
Angular spread [5]	5°
Number of TDP	4
Doppler characteristics	Classic
DOA & Time delay [10]	GBSBM
Base station noise figure	5dB
Base station antenna gain	13dBi
Mobile terminal noise figure	9dB
Mobile terminal antenna gain	0dBi
Target $\mathcal{E}_b/N_o$	10/6 dB
Coding	Convolutional rate 1/3
Decoding	Hard Viterbi

TABLE I
SIMULATION PARAMETERS

To guarantee an even system load, each sector is assigned the same number of users with the same resource allocation at the beginning of the simulation. Since the spatial distribution of the users influences the performance of the algorithms, each experiment is repeated for 50 different random user positions.

Measurements are taken for the mobile of interest. The SINR, number of coded and raw bit errors and base station transmission power (for the downlink) are extracted every timeslot for which the MOI is active.

For fair comparison of the algorithms, ideal power control is applied on both uplink and downlink so that the (long-term) average $\mathcal{E}_b/N_o$ is constant. We therefore compare the algorithms based on their capability to reduce spatial interference. Table I summarizes the simulation parameters.

B. Results

We first compare the algorithms presented in Section III with the best beam (BB) approach under different system load conditions and a RAKE receiver structure.

On the uplink, we also compare the algorithms to the more complex space-time multi-user detection (ST-MUD) receiver in [11]. Naturally it outperforms the other algorithms due to its ability to jointly detect the symbols transmitted and it is provided as a reference. Figure 4 illustrates the measured SINR and coded BER obtained on the uplink. The SINR results clearly show that SMI-BB (data) outperforms both DPA-BB and SB-BB. We can also observe that SMI-BB (mid) performs poorly in terms of SINR, due to the presence of multiple time-differentiable paths as explained in Section III-C. However, when we consider the *coded* BER, SMI-BB (mid) performs better than expected, indicating that the SINR may not always be a good measure of performance.

It is also interesting to note the regression in coded BER performance of the ST-MUD for low number of users in Fig. 4. This is in fact directly due to the implementation of the ST-MUD, which for simplicity considers the out-of-cell interferers as spatially and temporally white noise. However the out-of-cell interference tends to be more spatially colored when the system load is small. In contrast, a larger number of users creates a more spatially white interference, better handled by this ST-MUD.

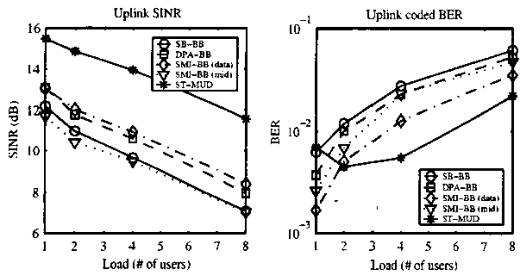

Fig. 4

UPLINK RESULTS

Alg.	Avg. DL Tx Power (dBm)
SB-BB	-24.59
DPA-BB	-25.44
SMI-BB (data)	-24.89
SMI-BB (mid)	-24.38

TABLE II

DOWNLINK TRANSMIT POWER (4 USERS)

On the downlink, the interference is due here to the other base stations. We observe that DPA-BB outperforms SB-BB significantly. In the SB approach, the base station on average makes an "error" in the direction of transmission because of the discrete nature of the switched beams. Because of this error, more transmission power is required than DPA-BB to obtained the same target $\mathcal{E}_b/N_o$, which in turns create more interference. This explains why the difference between SB-BB and DPA-BB increases with the load; each additional user contributes to the interference. Table II shows the average transmission power at the base station for each algorithm under a load of 4 users per sector. SB-BB requires on average 0.85 dB more power than DPA-BB to achieve the same target level at the mobile. SMI-BB is inappropriate on the downlink for the reasons outlined in Section III-C but performs relatively well here because the same allocation is used on the uplink and downlink.

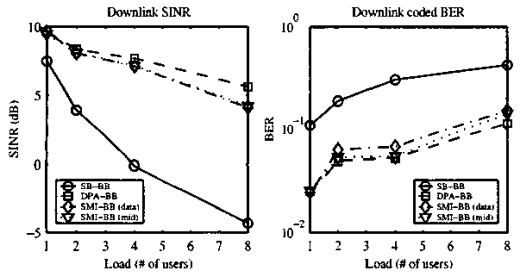

Fig. 5

DOWNLINK RESULTS

When using maximal ratio combining (MRC) on the uplink, we observe that the algorithms perform in general better than with the SB approach. As shown in Table III, a significant gain is obtained in coded BER when 2 beams are used (MRC (2)) compared to SB. The gain is marginal when increasing from 2 to 3 beams.

Alg.	BB	MRC ($N_b = 2$)	MRC ($N_b = 3$)
SB	0.0625	0.0171	0.0161
DPA	0.0534	0.0188	0.0192
SMI (data)	0.0349	0.0087	0.0071
SMI (mid)	0.0477	0.0213	0.0210

TABLE III

UPLINK CODED BER (4 USERS)

V. CONCLUSION

This paper compares three beamforming algorithms, namely switched beam, dynamically phased arrays and sample matrix inversion, in the context of a Third Generation cellular system. The results show that on the uplink SMI outperforms the other algorithms when the statistics are estimated not from the training sequence but directly from the data fields. For the downlink transmission, DPA performs significantly better than SB whereas SMI is not appropriate. The results also show that using multiple beams is advantageous and a significant gain is obtained when using a ST-MUD receiver structure instead of a RAKE in UTRA/TDD.

ACKNOWLEDGEMENT

We would like to thank InterDigital Canada Ltée and the Natural Sciences and Engineering Research Council of Canada (NSERC) for supporting this work.

REFERENCES

[1] B. Göransson, B. Hagerman, and J. Barta, "Adaptive antennas in WCDMA systems - link level simulation results based on typical user scenarios," in *Vehicular Technology Conference, 2000. IEEE VTC-Fall VTC 2000. 52nd*, vol. 1, 2000, pp. 157–164.

[2] G. Lehmann, C. Gessner, and M. Haardt, "Evaluation of link-level performance improvements by using smart antennas for the TD-CDMA based UTRA TDD mobile radio system," in *Vehicular Technology Conference, 2000. IEEE VTS-Fall VTC 2000. 52nd*, vol. 3, 2000, pp. 1328–1332.

[3] M. Haardt, A. Klein, R. Koehn, S. Oestreich, M. Purat, V. Sommer, and T. Ulrich, "The TD-CDMA based UTRA TDD mode," *IEEE Journal on Selected Areas in Communications*, vol. 18, no. 8, pp. 1375–1385, Aug. 2000.

[4] Third Generation Partnership Project (3GPP), "http://www.3gpp.org."

[5] A. Stéphenne and B. Champagne, "Effective multi-path vector channel simulator for antenna array systems," *IEEE Transactions on Vehicular Technology*, vol. 49, no. 6, pp. 2370–2381, Nov. 2000.

[6] L. C. Godara, "Application of antenna arrays to mobile communicaitons, part ii: Beam-forming and direction-of-arrival considerations," in *Proc. of IEEE*, vol. 85, 1997, pp. 1195 – 1245.

[7] J. Capon, "High-resolution frequency-wavenumber spectrum analysis," in *Proc. of IEEE*, vol. 57, 1969, pp. 2408 – 2418.

[8] R. O. Schmidt, "Multiple emmitter location and signal parameter estimation," in *IEEE Trans. on Antennas and Propagation*, vol. 34, 1989, pp. 276–280.

[9] R. Roy and T. Kailath, "ESPRIT - Estimation of Signal Parameter via Rotational Invariance Techniques," in *IEEE Trans. on Acoust. Speech, Signal Processing*, vol. 37, 1989, pp. 984 – 995.

[10] J. C. Liberti, Jr. and T. S. Rappaport, *Smart Antennas for Wireless Communications: IS-95 and Third Generation CDMA Applications*. Prentice Hall, 1999.

[11] M. Vollmer, M. Haardt, and J. Gotze, "Comparative study of joint-detection techniques for TD-CDMA based mobile radio systems," *IEEE Journal on Selected Areas in Communications*, vol. 19, no. 8, pp. 1461–1475, Aug. 2001.